Heat transfer modelling of encapsulated phase change materials for food packaging

Hong-Minh Hoang, Denis Leducq, R. Pérez Masia, J.M. Lagaron, G. Alvarez

▶ **To cite this version:**

Hong-Minh Hoang, Denis Leducq, R. Pérez Masia, J.M. Lagaron, G. Alvarez. Heat transfer modelling of encapsulated phase change materials for food packaging. 3rd IIR International Conference on Sustainability and the Cold Chain, ICCC 2014, Jun 2014, London, France. pp.405-411. hal-01469093

HAL Id: hal-01469093
https://hal.science/hal-01469093

Submitted on 16 Feb 2017

HAL is a multi-disciplinary open access archive for the deposit and dissemination of scientific research documents, whether they are published or not. The documents may come from teaching and research institutions in France or abroad, or from public or private research centers.

L'archive ouverte pluridisciplinaire **HAL**, est destinée au dépôt et à la diffusion de documents scientifiques de niveau recherche, publiés ou non, émanant des établissements d'enseignement et de recherche français ou étrangers, des laboratoires publics ou privés.

3rd IIR International Conference on Sustainability and the Cold Chain, ICCC 2014
23/06/2014 - 25/06/2014, London UK
pp. 405-411

HEAT TRANSFER MODELLING OF ENCAPSULATED PHASE CHANGE MATERIALS FOR FOOD PACKAGING

H.M. HOANG[a], D. LEDUCQ[a], R. PÉREZ-MASIA[b], J.M. LAGARON[b], G. ALVAREZ[a]
[a] Irstea, UR GPAN, 1 rue Pierre-Gilles de Gennes, 92761 Antony, France
Tel: 33 1 40 96 65 02, Fax: 33 1 40 96 60 75, e-mail: hong-minh.hoang@irstea.fr
[b] Novel Materials and Nanotechnology Group, Institute of Agrochemistry and Food Technology (IATA-CSIC), Avda. Agustin Escardino 7, 46980 Paterna (Valencia), Spain

ABSTRACT

Temperature abuses in cold chain can lead to deterioration in food quality and safety. Packaging can play an active role in temperature controlling of perishable products. However, standard materials for product packaging (plastic, cardboard or wood) usually have limited thermal buffering capacity. One possible approach to enhance this capacity and maintain the product at a desired temperature is thermal energy storage by phase change materials - PCM. In the present work, the heat transfer behaviour of a plate made from encapsulated PCM (Rubitherm RT5 encapsulated in polycaprolactone PCL) was studied. The enthalpy method was chosen to model the phase transition of the PCM. The model was validated by experimental cooling and heating processes, under controlled air temperature conditions. The numerical result demonstrated a better thermal capacitance of the encapsulated PCM material compared to a standard one (cardboard).

1. INTRODUCTION

In recent studies, encapsulated phase change materials (PCM) were developed as novel materials for food packaging because of their improved thermal capacitance. A PCM is a substance that undergoes a phase transition (e.g. fusion/crystallization) at a specific temperature or in a narrow range of temperature. It can have a high enthalpy of phase transition and then is capable of storing and releasing large amounts of energy (Rentas et al., 2004).
Chilled food products are often stored between 0 and 6°C; therefore, the PCM phase change temperature should be chosen in the temperature range of 4-8°C. The PCM is liquid at room temperature so its handling can become an issue for some applications. To limit its leakage while changing from the solid to the liquid state, the PCM should be contained in some recipient. One solution is to encapsulate the PCM inside a shell material (Cheng et al., 2012) or a nanostructured material (Pérez-Masiá et al., 2013). Among the encapsulation technologies, micro and nanoencapsulation prevent volatile losses, allow a greater dispersion and minimize the amount of non-encapsulated product. Electrospinning technique has been proven to be a suitable method for nanostructured encapsulation. Many compounds, including biomedical substances or functional food ingredients, have been encapsulated in polymeric matrices by means of this method (Goldberg et al., 2007; López-Rubio and Lagaron, 2012).
The aim of the present work is to study the heat transfer behaviour of a plate made from nanostructured encapsulated PCM material. The phase transition can be modelled by many methods based on the energy balance equation: tracking of the solid–liquid interface (Azzouz et al., 2008), enthalpy (Zhou et al., 2010; Melone et al., 2012) and apparent heat capacity (Antony Aroul Raj and Velraj, 2011). In this study, the enthalpy method was chosen. This method simplifies the solution of the phase change problem avoiding the explicit tracking of the solid–liquid interface.

2. MATERIALS AND METHODS

2.1. Encapsulated PCM materials

Rubitherm RT5 was selected as PCM material since it has a phase transition around 5ºC, a suitable temperature for chilled food keeping. PCM capsules were made through a high voltage spinning technology known as “electrospinning”. The process uses high voltage electric fields to produce electrically charged jets from viscoelastic polymer solutions which on drying, by the evaporation of the solvent, produce micro, submicro (also called ultrathin) or nanostructured polymeric structures. Particular details of the basic setup of

our spinning apparatus developed in-house were presented in Torres-Giner et al. (2009). A significant advantage of the technique is the suitable use of biomass-derived materials and of biodegradable polymers as encapsulating elements, with the corresponding environmental benefits. Different biopolymers were tested and finally polycaprolactone (PCL) was selected as the most suitable shell material, since this material was able to encapsulate the biggest amounts of PCM.
Different concentrations of polymer and PCM were tested in order to obtain the most efficient encapsulated systems in terms of encapsulation efficiency (defined as the percentage of PCM in the suspension with the polymer that goes into the capsules). The selected fibre mats were put together and lightly pressed using a hot-plate hydraulic press to form 0.5 to 1 cm thickness plates. In this study, a plate of 38% PCM mass fraction was tested. Its characteristics (density, heat capacity, heat conductivity, porosity …) were reported in the Table 1.

Table 1 – Properties of PCM encapsulated plate
(measured or calculated from pure materials properties)

Mass fraction of RT5	0.38	Source
Dimensions (m)	0.037 x 0.037 x 0.005	Measured
Mass (g)	2.68	Measured
Porosity	0.62	Calculated from the properties of pure materials
Density at 20°C (kgm^{-3})	356	
Density below the crystallization region (kgm^{-3})	378	
Heat capacity ($Jkg^{-1}K^{-1}$)	1755	
Heat conductivity ($Wm^{-1}K^{-1}$)	0.11	

2.2. Differential scanning calorimetry (DSC)

Differential scanning calorimetry (DSC) analyses were performed on a Perkin Elmer DSC 7 (US) under a nitrogen atmosphere using a subambient cooling accessory (Figure 1, DSC at the heat flow rate of 5°C/min). Analysis of a DSC thermogram enables the determination of two important parameters: the phase transition temperature range and the denaturation enthalpy (or phase change enthalpy - ΔH). Hysteresis was observed: the crystallization began at a lower temperature (about 4°C) compared to the end of the melting (about 8°C).

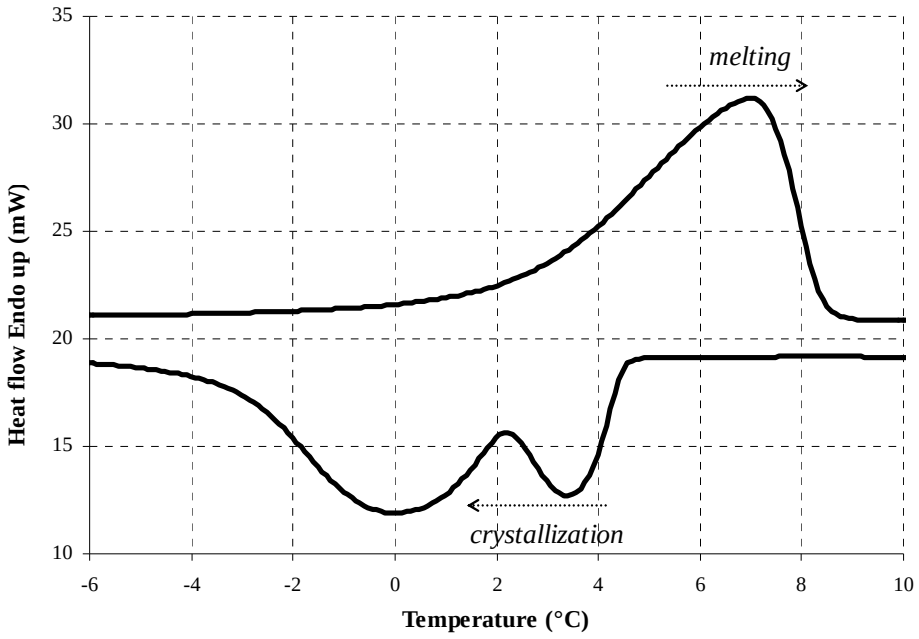

Figure 1: DSC result of the encapsulated PCM material

2.3. Heat transfer model development

The enthalpy model (Zhou et al., 2010) was applied to study the heat transfer phenomenon. The *y* dimension corresponds to the plate thickness: it was assumed that the plate thickness (E) is a lot smaller than its length and width so that the 1D model can be used.

$$\rho \frac{\partial H(y,t)}{\partial t} = \frac{\partial}{\partial y}\left(k \frac{\partial T(y,t)}{\partial y} \right) \qquad 0 \le y \le E \tag{1}$$

The enthalpy H is in function of the temperature T as:

$$H = \begin{cases} \int_{T0}^{T} c_{p,s}\, dT & when\ \ T < T1 \\ \int_{T0}^{T1} c_{p,s}\, dT + \int_{T1}^{T} c_{p,PC}\, dT & when\ \ T1 < T < T2 \\ \int_{T0}^{T1} c_{p,s}\, dT + \int_{T1}^{T2} c_{p,PC}\, dT + \int_{T1}^{T} c_{p,l}\, dT & when\ \ T > T2 \end{cases} \tag{2}$$

where: *T0* is the reference temperature where $H(T0) = 0$,

[*T1, T2*] is the temperature range in which the phase transition occurs

$c_{p,s}$, $c_{p,PC}$, $c_{p,l}$ are the heat capacities of the solid, phase transition and liquid states

Figure 2 shows the enthalpy evolution in function of temperature in which the three states (liquid, phase transition and solid) can be easily identified; the greater change of enthalpy corresponds to the phase change region.

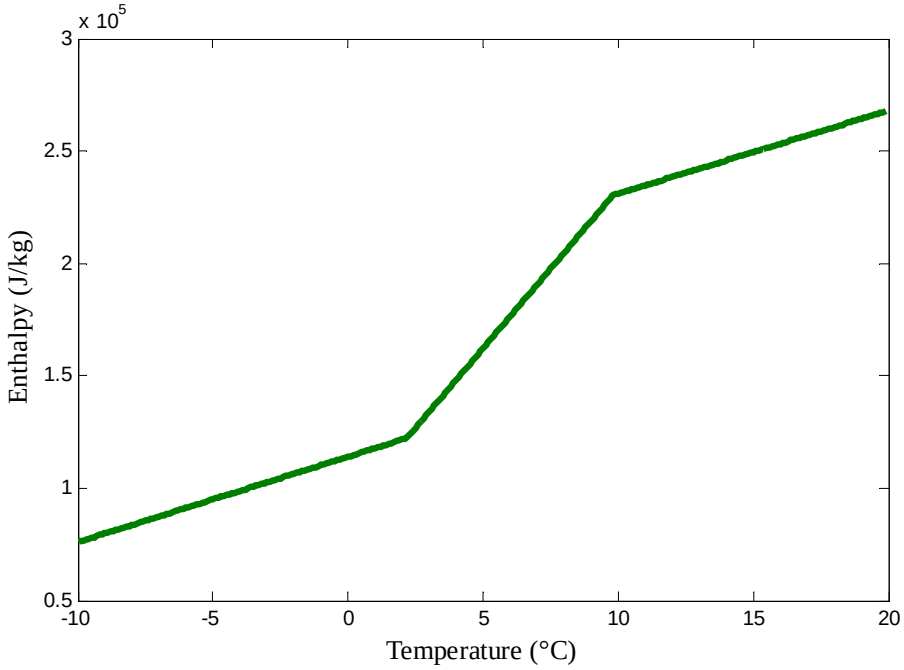

Figure 2: Enthalpy in function of temperature

The plate's properties (density, heat capacity, heat conductivity…) are considered to be spatially homogeneous, i.e. no heterogeneous structure caused by the polymers, PCM and air distribution are considered.

The initial condition at time *t=0* was considered as:

$$T(y,t=0))=T_0(y) \tag{3}$$

The convective heat transfer boundary condition was applied at the surface:

$$k\left.\frac{\partial T}{\partial y}\right|_{y=0} = h(T_a - T(y=0,t)) \tag{4}$$

The equation system (eq. 1 to 4) was solved numerically using the finite volume method coupled with the fully implicit finite difference scheme. The spatial and temporal domains were discretized uniformly in M grids ($1 \le i \le M$) and N time steps ($1 \le n \le N$) (Figure 3). The discretized equation system takes the following form:

$$\begin{cases} for\ \ i=1\&M \\ T_i^{n+1}=\left(T_a^{n+1}+\dfrac{k}{h\Delta y/2}T_2^{n+1}\right)\Big/\left(1+\dfrac{k}{h\Delta y/2}\right) \\ H_i^{n+1}=enthalpy\_function\left(T_i^{n+1}\right) \\ \\ for\ \ (i=2,j=3)\ \ \&\ \ (i=M-1,j=M-2) \\ H_i^{n+1}=H_i^n+\dfrac{\Delta t}{\rho\Delta y^2}\left[kT_j^{n+1}-\left(k+\dfrac{1}{1/(h\Delta y)+1/(2k)}\right)T_j^{n+1}+\dfrac{T_a^{n+1}}{1/(h\Delta y)+1/(2k)}\right] \\ T_i^{n+1}=inverse\_enthalpy\_function(H_i^{n+1}) \\ \\ for\ \ 3\le i\le M-2 \\ H_i^{n+1}=H_i^n+\dfrac{k\Delta t}{\rho\Delta y^2}\left(T_{i+1}^{n+1}+T_{i-1}^{n+1}-2T_i^{n+1}\right) \\ T_i^{n+1}=inverse\_enthalpy\_function(H_i^{n+1}) \end{cases} \tag{5}$$

The *'enthalpy_function'* corresponds to eq.2 and the *'inverse_enthalpy_function'* is its inverse form.

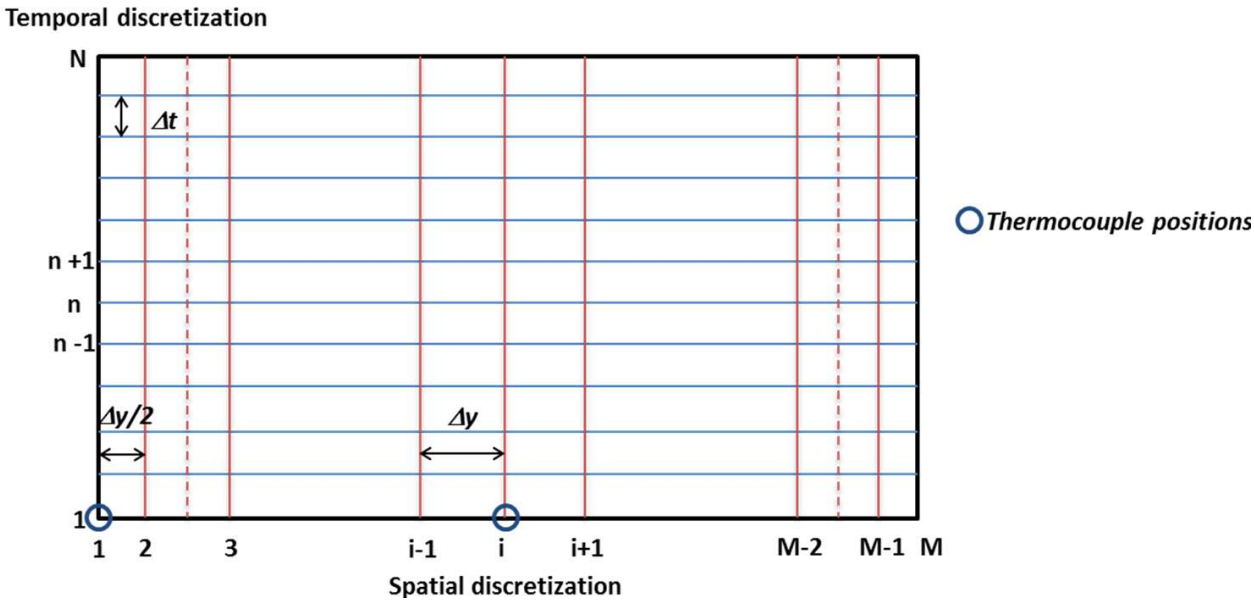

Figure 3: Schema of the finite volume model with the positions of the thermocouples used for model validation

Note that the system (5) resolves both enthalpy and temperature at each time step. This system is numerically solved by using over relaxation iteration algorithm (Zhou et al., 2010) with a relaxation factor of 1.5. When the enthalpy difference between two iterations $\sum_{i=1}^{M}\left(\Delta H_i^n\right)^2$ is less than the given precision $\left(0.0001 Jkg^{-1}\right)$, the obtained enthalpy and temperature are recorded and the calculation proceeds to the next time step. The spatial grid size is 0.00028 m and the time step is 0.1 s. Further refinement of either space grid and time steps shows no effect on the results.

2.4. Experimental validation

Experiments were carried out inside a temperature simulator in order to study the temperature evolution of the plate during heating and cooling process. T-type thermocouples (1 mm diameter, precision ±0.2°C) were inserted in the plate's center and surface to measure its temperature. Air temperature near the plate was also measured. These thermocouples were previously calibrated at 5 different temperatures (-25°C, -15°C, 0°C, +15°C and +25°C).

During the experiments, the air temperature inside the simulator was maintained constant. The convective heat transfer coefficient (around 10 $W.m^{-2}.K^{-1}$) was measured using an aluminium heating object. Maximum attention was taken to obtain a homogeneous initial temperature for the plate. For heating experiment (plate initial temperature -10°C, air temperature in the simulator 20°C), the plate was kept inside a home freezer at -10°C for at least 12h. For cooling experiment (plate initial temperature 17°C, air temperature in the simulator -10°C), the plate was kept at ambient temperature. When the plate was moved to the simulator, it was packed inside an insulated box. Therefore, the initial center and surface temperatures were almost the same (<0.5°C of difference).

3. RESULTS AND DICUSSION

3.1. Comparison between experimental and numerical results

Figure 4 shows a comparison between experimental and numerical results of the plate's temperature evolution during heating and cooling processes. For both processes, the phase change occurred between -2°C and 10°C and stayed for around 500s, offering a better thermal capacitance for the material in this range of temperature. The hysteresis was observed, the melting began at a higher temperature (2°C) compared to the end of the crystallization (-2°C) which agreed with the DSC results. It can be observed that the model under predicts the surface temperature during the heating process and over predicts the surface temperature during the cooling process. The difference may relate to the precision of the model input parameters (thermal properties, heat transfer coefficient …). The plate center temperature, however, was relatively well predicted (maximum difference < 1.2°C) for both heating and cooling processes.

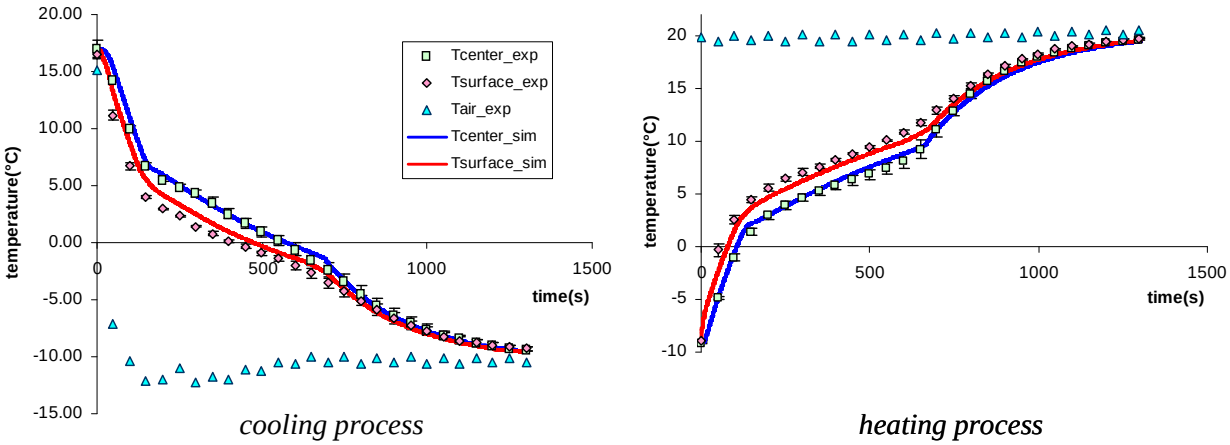

Figure 4: Comparison between experimental and numerical results of the temperature evolution of the plate during heating and cooling processes

Note: the model developed in this study simulates separately cooling and heating processes because of important hysteresis during thermal cycling (Figure 1). In fact, two different enthalpy functions (eq.2) were developed for each process (heating or cooling).

3.2. Thermal capacitance of encapsulated PCM

In order to study the thermal capacitance of the encapsulated PCM material, a numerical simulation was carried out in which the encapsulated PCM plate, initially at 2°C, was submitted to a temperature spike of 20°C during 100 s. The plate temperature evolution was compared to the one of a cardboard plate of the same dimensions; the result was shown in Figure 5. Because of the temperature spike, the PCM temperature increased up to 5°C at the plate's surface and 4°C at the plate's center. The cardboard plate temperature, however, attained 17°C. This result demonstrated the better thermal capacitance of the encapsulated PCM material compared to a standard one.

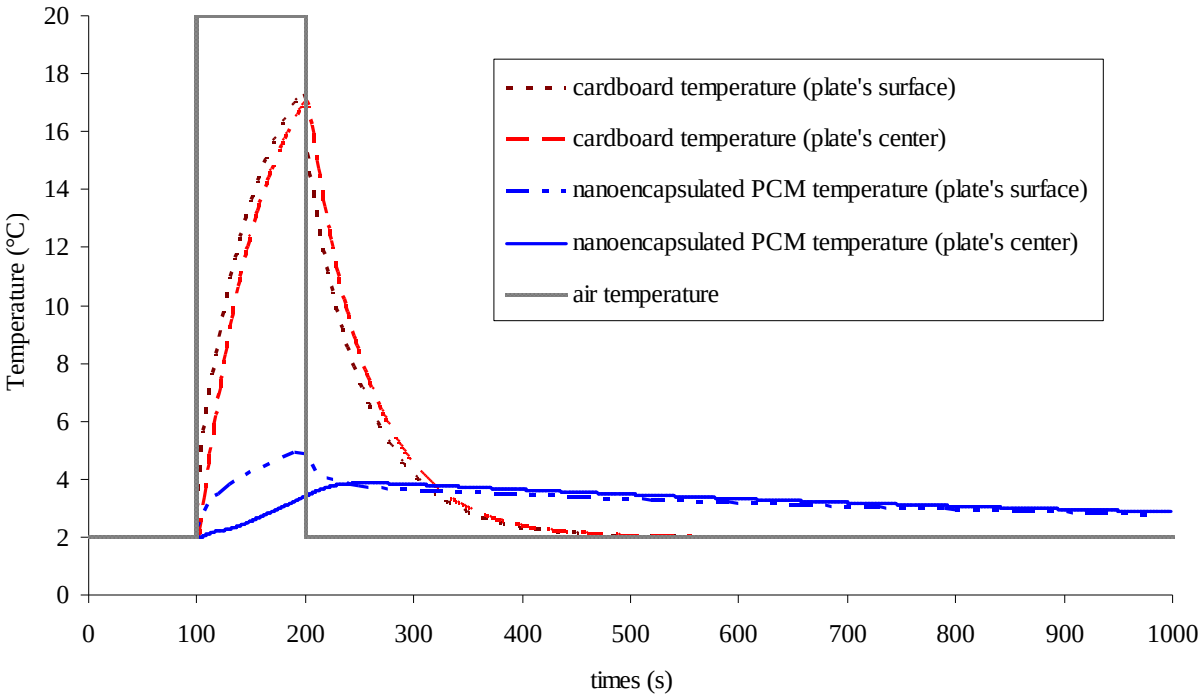

Figure 5: Temperature evolution of nanoencapsulated PCM and cardboard plates during a temperature spike

4. CONCLUSION

A model of heat transfer for encapsulated PCM material (RT5 – PCL) was developed. It takes into account the variation of thermal properties in function of temperature and the phase change of the PCM material by the enthalpy method. The validation of the model was carried out by experiments during heating and cooling processes. The results showed that this material has a better thermal capacitance between -2°C and 10°C compared to a standard packaging material which can enhance the thermal protection of perishable products.

ACKNOWLEDGEMENT

The research leading to this result has received funding from European Community's Seventh Framework Programme (FP7/2007-2013) under the grant agreement n° 245288.

NOMENCLATURE

c_p	heat capacity	($J.kg^{-1}.K^{-1}$)
E	plate thickness	(m)
h	heat transfer coefficient	($W.m^{-2}.K^{-1}$)
k	heat conductivity	($W.m^{-1}.K^{-1}$)
M	number of mesh points	(-)
t	time	(s)
T	temperature	(°C)
y	dimension of the plate thickness	(m)
ρ	density	($kg.m^{-3}$)

Subscripts

a	air
l	*liquid*
PC	*phase change*
s	*solid*

REFERENCES

1. Antony Aroul Raj V., Velraj R. , 2011. Heat transfer and pressure drop studies on a PCM-heat exchanger module for free cooling applications. *International Journal of Thermal Sciences,* 50,(8), 1573-1582.
2. Azzouz K., Leducq D., Gobin D., 2008. Performance enhancement of a household refrigerator by addition of latent heat storage. *International Journal of Refrigeration,* 31,(5), 892-901.
3. Cheng W.-l., Liu N., Wu W.-f., 2012. Studies on thermal properties and thermal control effectiveness of a new shape-stabilized phase change material with high thermal conductivity. Applied Thermal Engineering, 36,(0), 345-352.
4. Goldberg M., Langer R., Jia X., 2007. Nanostructured materials for applications in drug delivery and tissue engineering. *Journal of Biomaterials Science, Polymer Edition,* 18,(3), 241-268.
5. López-Rubio A., Lagaron J.M., 2012. Whey protein capsules obtained through electrospraying for the encapsulation of bioactives. *Innovative Food Science & Emerging Technologies,* 13,(0), 200-206.
6. Melone L., Altomare L., Cigada A., De Nardo L., 2012. Phase change material cellulosic composites for the cold storage of perishable products: From material preparation to computational evaluation. *Applied Energy,* 89,(1), 339-346.
7. Pérez-Masiá R., López-Rubio A., Lagarón J.M., 2013. Development of zein-based heat-management structures for smart food packaging. *Food Hydrocolloids,* 30,(1), 182-191.
8. Rentas F. J., Macdonald V. W., Houchens D. M., Hmel P. J., Reid T. J. , 2004. New insulation technology provides next-generation containers for "iceless" and lightweight transport of RBCs at 1 to 10°C in extreme temperatures for over 78 hours. *Transfusion,* 44,(2), 210-216.
9. Torres-Giner S., Ocio M.J., Lagaron J.M., 2009. Novel antimicrobial ultrathin structures of zein/chitosan blends obtained by electrospinning. *Carbohydrate Polymers,* 77,(2), 261-266.
10. Zhou G., Yang Y., Wang X., Cheng J., 2010. Thermal characteristics of shape-stabilized phase change material wallboard with periodical outside temperature waves. *Applied Energy,* 87,(8), 2666-2672.